NRL Memorandum Report 5172

Limitations on the Applicability of High-Explosive Charges for Simulating Nuclear Airblast

D. BOOK, D. FYFE, M. PICONE, AND M. FRY*

Laboratory for Computational Physics

**Science Applications Inc.*
McLean, VA 22102

September 22, 1983

This work was supported by the Defense Nuclear Agency under Subtask N99QAXAH. work unit 00061 and work unit title "Cloud Calculations."

NAVAL RESEARCH LABORATORY
Washington, D.C.

SECURITY CLASSIFICATION OF THIS PAGE (When Data Entered)

REPORT DOCUMENTATION PAGE	READ INSTRUCTIONS BEFORE COMPLETING FORM
1. REPORT NUMBER: NRL Memorandum Report 5172	2. GOVT ACCESSION NO.: AD-A133 368
3. RECIPIENT'S CATALOG NUMBER	
4. TITLE (and Subtitle): LIMITATIONS ON THE APPLICABILITY OF HIGH-EXPLOSIVE CHARGES FOR SIMULATING NUCLEAR AIRBLAST	5. TYPE OF REPORT & PERIOD COVERED: Interim report on a continuing NRL problem.
	6. PERFORMING ORG. REPORT NUMBER
7. AUTHOR(s): D. Book, D. Fyfe, M. Picone, and M. Fry*	8. CONTRACT OR GRANT NUMBER(s)
9. PERFORMING ORGANIZATION NAME AND ADDRESS: Naval Research Laboratory, Washington, DC 20375	10. PROGRAM ELEMENT, PROJECT, TASK AREA & WORK UNIT NUMBERS: 62715H; 44-1912-A-3
11. CONTROLLING OFFICE NAME AND ADDRESS: Defense Nuclear Agency, Washington, DC 20305	12. REPORT DATE: September 22, 1983
	13. NUMBER OF PAGES: 37
14. MONITORING AGENCY NAME & ADDRESS(if different from Controlling Office)	15. SECURITY CLASS. (of this report): UNCLASSIFIED
	15c. DECLASSIFICATION/DOWNGRADING SCHEDULE

16. DISTRIBUTION STATEMENT (of this Report)

Approved for public release; distribution unlimited.

17. DISTRIBUTION STATEMENT (of the abstract entered in Block 20, if different from Report)

18. SUPPLEMENTARY NOTES

*Present address: Science Applications Inc., McLean, VA 22102.

This work was supported by the Defense Nuclear Agency under Subtask N99QAXAH, work unit 00061, and work unit title "Cloud Calculations."

19. KEY WORDS (Continue on reverse side if necessary and identify by block number)

Explosions
Blast waves
Chemical explosive
Nuclear explosion
Fireball
Airblast

20. ABSTRACT (Continue on reverse side if necessary and identify by block number)

Since the flow fields that result from nuclear and high explosive (HE) detonations are qualitatively alike but quantitatively different, consequently care must be exercised in carrying over conclusions drawn from measurements of HE tests to nuclear explosions. The usefulness of HE explosions for simulating nuclear airblast is predicated on the fact that after reaching 5-6 times the initial radius the flow field looks like that produced by a point source and produces shock overpressures simular to those in the nuclear case. Numerical simulations of airblast phenomena have been carried out using one- and two-fluid

(Continues)

DD FORM 1 JAN 73 1473 EDITION OF 1 NOV 65 IS OBSOLETE
S/N 0102-014-6601

SECURITY CLASSIFICATION OF THIS PAGE (When Data Entered)

20 ABSTRACT (Continued)

Flux-Corrected Transport hydrodycodes in one and two dimensions. The principal difference in the free-field solutions are the presence in the HE case of a contact discontinuity between air and HE products and of a backward-facing shock behind it. Temperatures in the nuclear fireball are initially three orders of magnitude higher; correspondingly, the density minimum at the center of the fireball is much broader and deeper. When the blast wave in a nuclear height-of-burst (HOB) situation undergoes regular reflections from the ground only one peak develops in the overpressure, and the reflected wave propagates upward rapidly through the hot underdense fireball. In the HE case part of the upward-moving reflected wave is reflected downward at the contact surface, producing a second pressure peak on the ground, while the shock transmitted through the contact surface propagates slowly upward. After transition to Mach reflection other differences appear. At late times following shock breakaway the nuclear fireball, unlike the HE fireball, appears to develop a Rayleigh-Taylor instability along its lower edge below the HOB. The vortices (both forward and reverse) are stronger and form earlier. This has important consequences for fireball rise and for dust entrainment and transport to high altitudes.

CONTENTS

LIMITATIONS ON THE APPLICABILITY OF HIGH-EXPLOSIVE CHARGES FOR SIMULATING NUCLEAR AIRBLAST

D. Book, D. Fyfe, M. Picone, Naval Research Laboratory, Washington, D.C.

M. Fry, Science Applications, Inc., McLean, Virginia

The flow fields that result from nuclear and high explosive (HE) detonations are qualitatively alike but quantitively different. Consequently, care must be exercised in carrying over conclusions drawn from measurements of HE tests to nuclear explosions. The usefulness of HE explosions for simulating nuclear airblast is predicated on the fact that after reaching 5-6 times the initial radius the flow field looks like that produced by a point source and produces shock overpressures similar to those in the nuclear case. Numerical simulations of airblast phenomena have been carried out using one- and two-fluid Flux-Corrected Transport hydrocodes in one and two dimensions. The principal differences in the free-field solutions are the presence in the HE case of a contact discontinuity between air and HE products and of a backward-facing shock behind it. Temperatures in the nuclear fireball are initially three orders of magnitude higher; correspondingly, the density minimum at the center of the fireball is much broader and deeper. When the blast wave in a nuclear height-of-burst (HOB) situation undergoes regular reflection from the ground only one peak develops in the overpressure, and the reflected wave propagates upward rapidly through the hot underdense fireball. In the HE case

Manuscript approved June 29, 1983.

part of the upward-moving reflected wave is reflected downward at the contact surface, producing a second pressure peak on the ground, while the shock transmitted through the contact surface propagates slowly upward. After transition to Mach reflection other differences appear. At late times following shock breakaway the nuclear fireball, unlike the HE fireball, appears to develop a Rayleigh-Taylor instability along its lower edge below the HOB. The vortices (both forward and reverse) are stronger and form earlier. This has important consequences for fireball rise and for dust entrainment and transport to high altitudes.

Section 1
INTRODUCTION

In this paper we describe a series of calculations carried out as part of the ongoing NRL effort aimed at studying airblast effects. The phenomena of chief interest to us include the following: peak overpressures and pressure histories on the ground as functions of yield, range, and height of burst (HOB), both at early times (prior to and during transition to Mach reflection) and at late times (after shock breakaway, with peak pressure in the range of tens of psi); velocity fields, particularly those associated with the toruses (both forward and reverse) in the neighborhood of the rising fireball; and the distribution of dust lifted off the ground by the winds and the structure of the cloud at the time of stabilization. We are interested in comparing the nuclear and HE cases, and learning how much they differ from one another. Our motivation is to determine the extent to which HE tests can simulate events in a nuclear height-of-burst situation.

The technique we have employed for this purpose is numerical modeling. One- and two-fluid hydrocodes based on the Flux-Corrected Transport (FCT) shock-capturing techniques[1] have been used to simulate airblast phenomena in one and two dimensions. FCT refers to a class of state-of-the-art fluid computational algorithms developed at NRL in the course of the past ten years with supersonic gas-dynamic applications expressly in mind. Simply put, our procedure is to model a one-kton nuclear burst and its 600-ton chemical equivalent, both at a HOB of 50 m, and compare the results. In order to validate, initialize, and interpret these 2D simulations, a number of ancillary calculations (mostly 1D) were undertaken. The results are most conveniently exhibited in terms of plots of peak overpressure vs range and time, station histories, contour plots of combustion product and total density, velocity vector plots, and tracer particle trajectories. Examples of these are presented to illustrate our results and conclusions.

The plan of the paper is as follows: In the next section we discuss our numerical techniques and validation procedures. In Section 3 we discuss the free-field (1D) solution and indicate the salient differences between nuclear and HE cases. Section 4 describes the 2D HOB calculations done for the HE and nuclear cases. In Section 5 we summarize our conclusions and discuss their domain of validity. We find that simulation of nuclear explosions by HE has distinct limitations, particularly at early times, in the fireball and transition regions, and in the details of the dust scouring process.

Section 2
NUMERICAL TREATMENT

FCT is a finite-difference technique for solving the fluid equations in problems where sharp discontinuities arise (e.g., shocks, slip surfaces and contact surfaces).[1] It modifies the linear properties of a second- (or higher-) order algorithm by adding a diffusion term during convective transport, and then subtracting it out "almost everywhere" in the antidiffusion phase of each time step. The residual diffusion is just large enough to prevent dispersive ripples from arising at the discontinuity, thus ensuring that all conserved quantities remain positive. FCT captures shocks accurately over a wide range of parameters. No information about the number or nature of the surfaces of discontinuity need be provided prior to initiating the calculation.

The FCT routine used in the present calculations, called JPBFCT (an advanced version of ETBFCT)[2], consists of a flexible, general transport module which solves 1-D fluid equations in Cartesian, cylindrical, or spherical geometry. It provides a finite-difference approximation to conservation laws in the general form:

$$\frac{\partial}{\partial t}\int_{\delta V(t)} \phi dV = -\int_{\delta A(t)} \phi(\underline{u}-\underline{u}_g)\cdot d\underline{A} + \int_{\delta A(t)} \tau dA, \qquad (1)$$

where ϕ represents the mass, momentum, energy or mass species in cell $\delta V(t)$, $\underline{u}$ and $\underline{u}_g$ represent the fluid and grid velocities, respectively, and τ represents the pressure/work terms. This formulation allows the grid to slide with respect to the fluid without introducing any additional

numerical diffusion. Thus, knowing where the features of greatest interest are located, one can concentrate fine zones where they will resolve these features most effectively as the system evolves.

The same transport routine is employed in the 2D r-z code (called FAST2D) via coordinate splitting. A Jones-Wilkins-Lee (JWL) equation of state (EOS) was used for the detonation products and a real-air EOS was used outside the HE-air interface.[3] The routine was written in the form of a table lookup, using interpolation with logarithms to the base 16 computed by means of logical shifts.[4] By thus taking account of the architecture of the machine (in these calculations, a 32-bit-word two-pipe Texas Instruments ASC) it was possible to generate very efficient vector code, decreasing the time required for EOS calculations to a small fraction of that required for the hydro. The EOS specifies pressure as a function of density and internal energy. In mixed cells the combined pressure was calculated according to Dalton's law.

For the HE calculations the initial conditions were taken to be the self-similar flow field corresponding to a spherical Chapman-Jouguet detonation at the time the detonation wave reaches the charge radius (Fig. 1)[3]. This was propagated with the 1D spherical code until the detonation front attained a radius just smaller than the HOB, at which time the solution was laid down on the 2D mesh (Fig. 2). The nuclear calculation was initialized with the 1-kton standard[5] with the same initial radius.

The boundary conditions were chosen to enforce perfect reflection on the ground and on the axis of symmetry

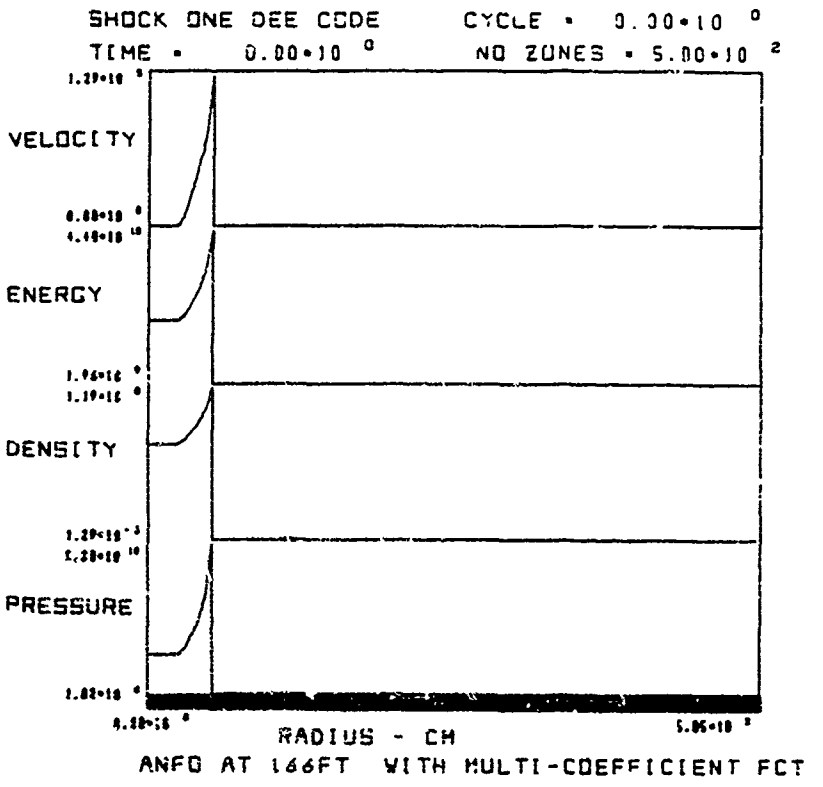

Figure 1

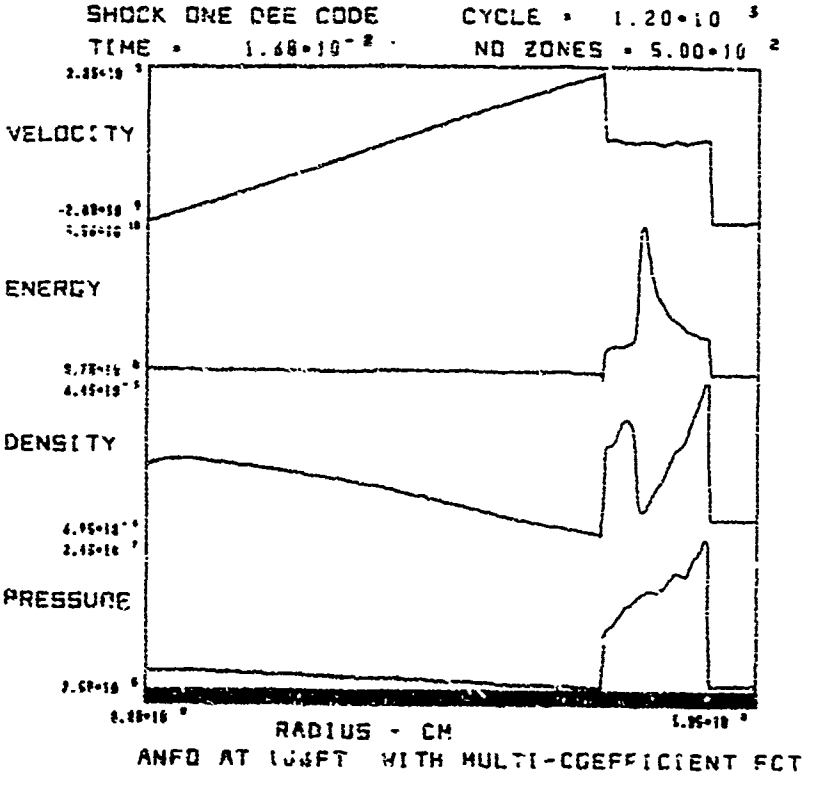

Figure 2

$[(d\phi/dn)_{bc} = 0$, where $\phi = \rho,p,v^t$, and $v^n_{bc} = 0]$, where "t" and "n" denote tangential and normal components, respectively, and outflow on the outer and the top boundaries $[(d\phi/dn)_{bc} = 0$, where $\phi = \rho,p,v^t,v^n]$.

For the 2D calculations the mesh was typically ~100 x 100. Fixed gridding was used to minimize numerical errors. These zones were 2.1 m x 2.1 m. For the late time calculations, a fixed mesh with 100 zones in the radial and 200 zones in the vertical direction was used, with all cells of dimension 4.2 m x 4.2 m.

Section 3
FREE-FIELD SOLUTION

The well-known Sedov similarity solution[6] for a point blast consists of a strong shock (post-shock pressure much larger than ambient pressure) followed by a rarefaction wave (Fig. 3). The density distribution is extremely concave and approaches zero at the origin. The pressure approaches a constant as $r \to 0$, so that the temperature diverges strongly. The profiles of the 1-kton standard solution (Fig. 4) are qualitatively similar, the temperature being essentially flat in the fireball region.

The solution used to initialize the HE problem, however, contains a number of features which are absent in the other solutions. These are most conspicuous in the density profile (Fig. 2), which exhibits a contact discontinuity between the HE products and shocked air, a secondary

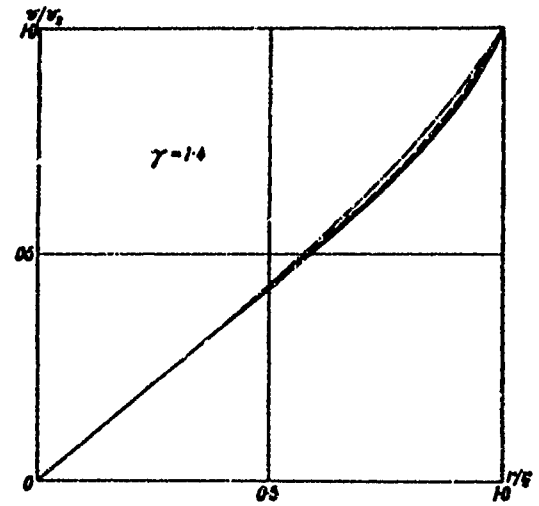

Velocity distribution behind the shock wave ——— spherical case; – – – – – cylindrical case; –·–·–·– plane case.

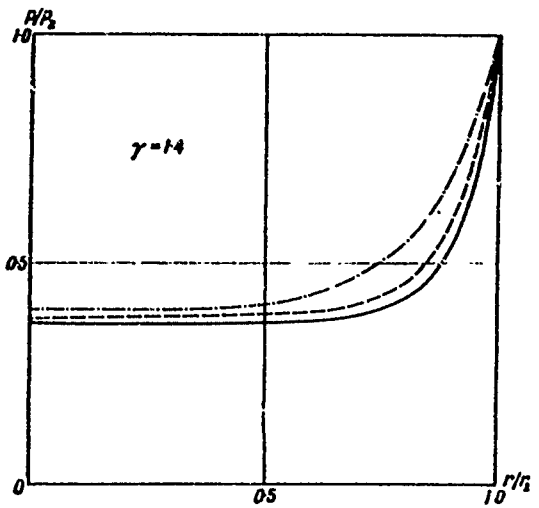

Pressure distribution behind the shock wave ——— spherical case; – – – – – cylindrical case; –·–·–·– plane case.

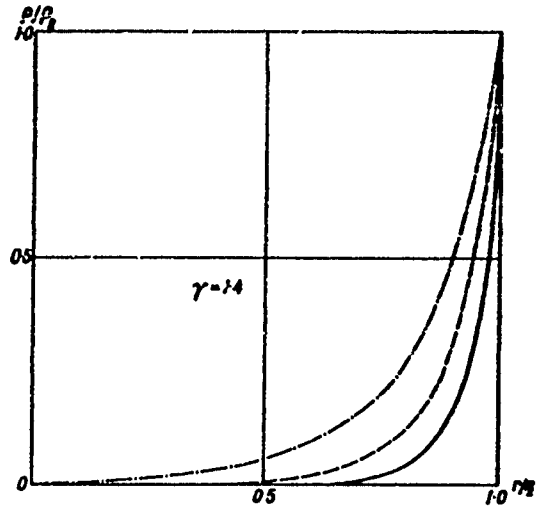

Density distribution behind the shock wave.

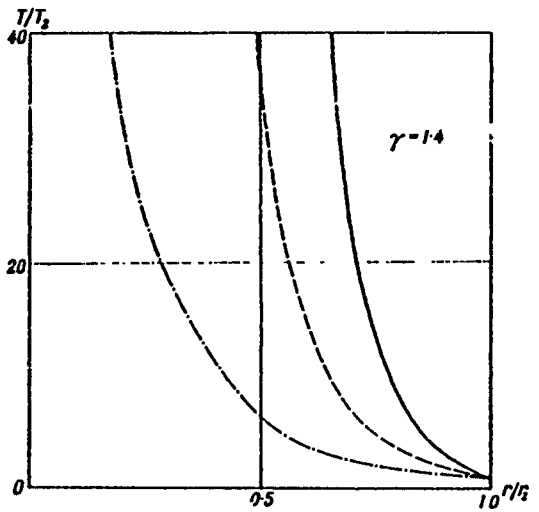

Temperature distribution behind the shock wave.

Figure 3

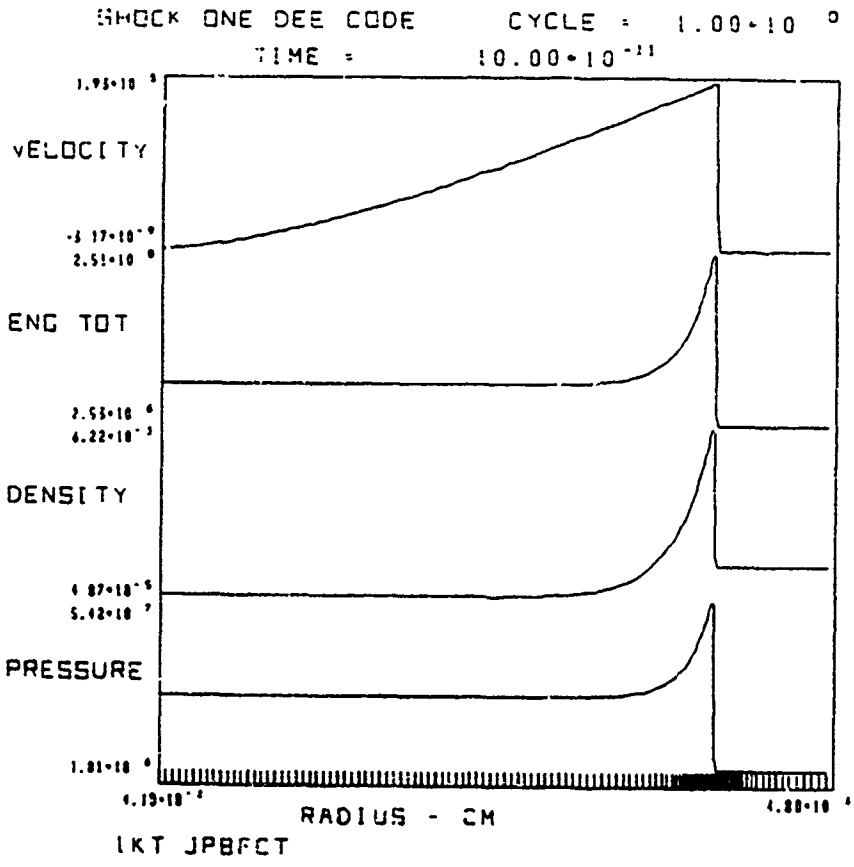

Figure 4

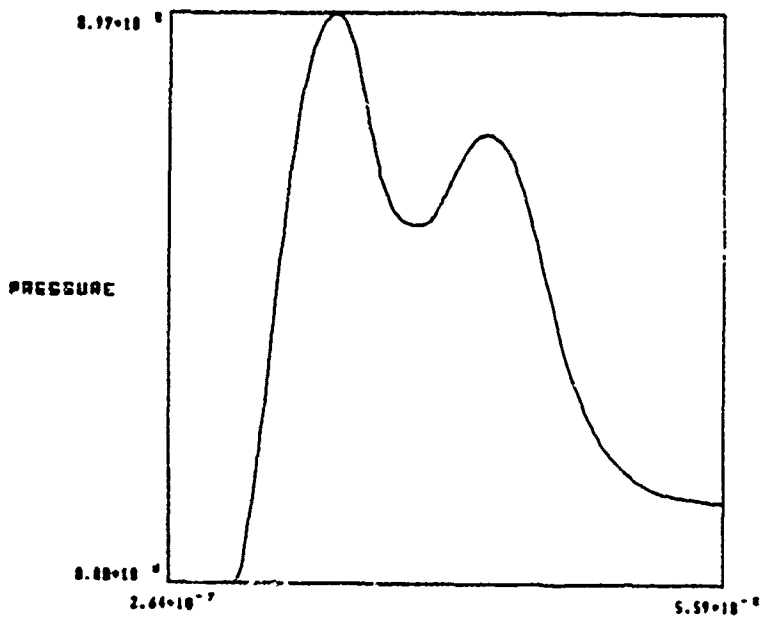

Figure 5

shock facing inward within the detonation products, and a gentle maximum near the origin. Because of this last feature, temperatures are about three orders of magnitude smaller in the fireball than in the nuclear case, and are nowhere divergent.

It follows that the speed of sound in the nuclear fireball is much greater than in the HE fireball. This has two immediate consequences, one physical and one numerical. The first is that shocks propagating through the nuclear fireball travel much faster. The second is that the upper limit on the computational timestep, set by the Courant criterion

$$\max \left(\frac{|v|+c}{\delta x}\,\delta t\right) < 1, \qquad (2)$$

which usually is determined by conditions in the fireball, is much smaller relative to the shock time scale $\tau_s = HOB/v_{shock}$ in the nuclear case than in the HE case.

As a result, even though the leading shock is well resolved (over ~ 2 zones) in the free-field solution, the process of reflection even at ground zero (where the shock is incident normally) takes hundreds of timesteps. Coupled with the property of FCT (known as "clipping") which makes the points of all sharply-peaked profiles tend to flatten out until they are > 3 zones across, this makes the rise time of the reflected shock quantities ~ 10 times longer than that of the incident shock. This can be seen using a 1D spherical model calculation (Fig. 4), as well as in oblique reflection in 2D. This spreading is a problem only while the shock is in the immediate vicinity of the reflecting boundary. After

the reflected shock has propagated a few zones back into the interior of the mesh, the profiles steepen up and assume their correct forms (this has been shown by rerunning the calculation with a refined mesh and comparing the peak values after reflection with those predicted theoretically).

When the reflected shock begins propagating back to the origin it encounters drastically different conditions in the HE and nuclear cases. In the former, it strikes the contact discontinuity where it is partly transmitted and partly reflected. The reflected shock then proceeds outward until it reaches the ground (the end of the grid in the 1D calculation), producing the second peak in the station history shown in Fig. 5. In contrast, the shock wave reflected from the ground passes unhindered through the fireball at high speed until it reaches the upper boundary of the fireball whereupon it reflects back.

As we shall show, it is primarily through these reverberating shock waves and the wind pattern they set up that the HE and nuclear HOB airblasts differ.

Section 4
2D SIMULATION OF AIRBLAST

The yield and HOB (600 tons and 166 ft, respectively) were chosen to equal the values used in the Direct Course experiment, which we are simulating. The Chapman-Jouguet parameters used to initialize the spherical free-field calculation were taken to be those for the NH_4NO_3-fuel oil (ANFO) mixture used as the explosive.

Figures 6(a)-(c) show the contours of HE density and internal energy per unit mass and the velocity arrow plot at t=0, just before the reflection at ground zero occurs. Figures 6(d)-(f) show the corresponding plots 54 ms later, while Figs. 6(g)-(i) show them after 245 ms. Note the reflected shock proceeding upward, reflecting again off the fireball, and propagating back in a downward and outward direction. The interaction of this shock with the radially inward flow near the ground generates the reverse vortex, which is clearly seen in Fig. 6(i). Note also the positive vortex forming near the top of the grid in the same plot. The latter results when the upward-propagating reflected shock interacts with the radially outward flow near the top of the fireball; it is not produced by the buoyant rise of the fireball, which at these early times has scarcely begun.

To look at the evolution of the fireball at late times, we reinitialized on a larger, coarser grid, representing a cylinder 400 m in radius and 800 m high. The first 300 cycles approximately reproduce the early-time results. The spherical shock breaks away and leaves the mesh. The flows remaining on the grid are now subsonic everywhere. Then the fireball begins to rise and the subsequent development is due to the combination of buoyant rise and the action of the vortices set up by the early shocks.

Figures 7(a)-(b) show the reaction product density and velocities at 0.93 s. Note the "toe" reaching out along the ground and the bulge near the bottom of the HE product density produced by the constructive interference of forward and reverse vortices. These features are accentuated with the passage of time; in Figs. 7(c)-(d) (t = 2.70 s), they are

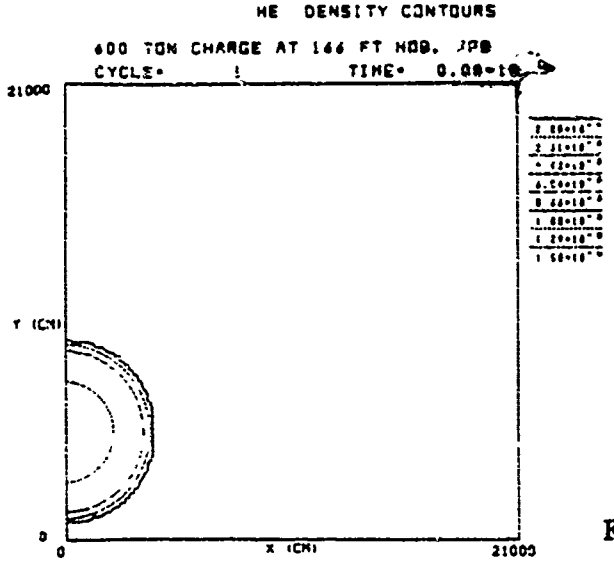

Figure 6a

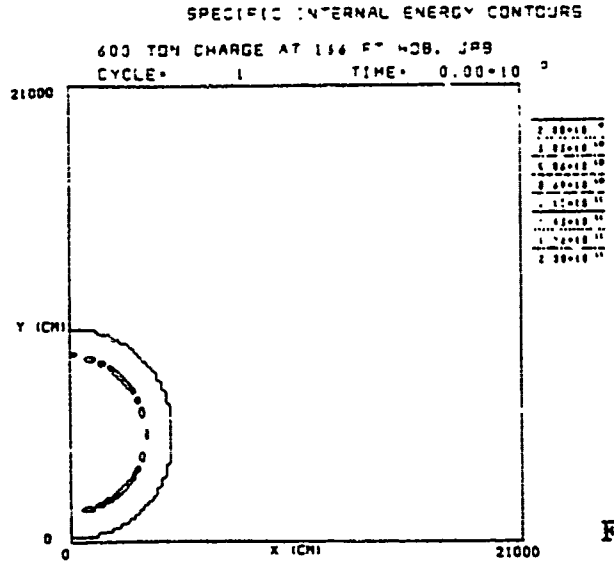

Figure 6b

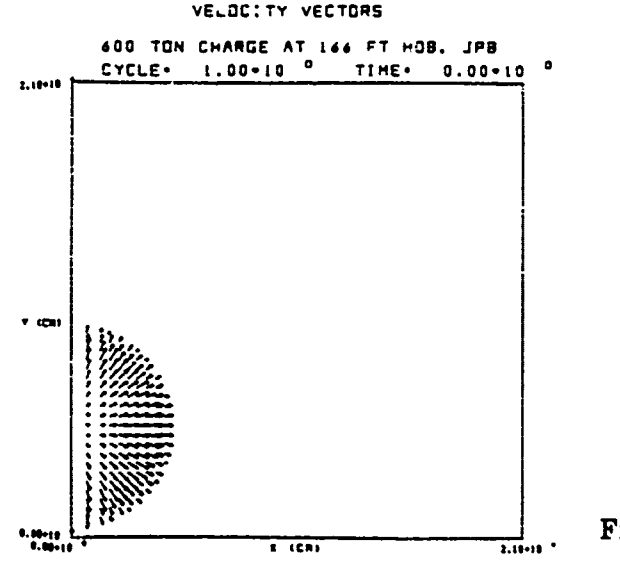

Figure 6c

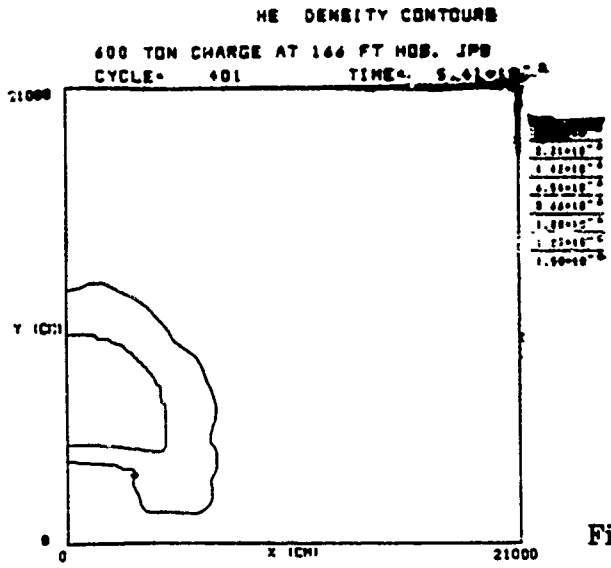

Figure 6d

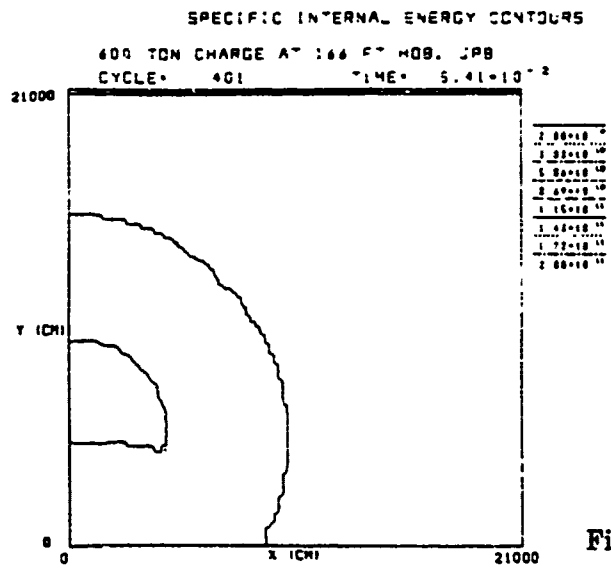

Figure 6e

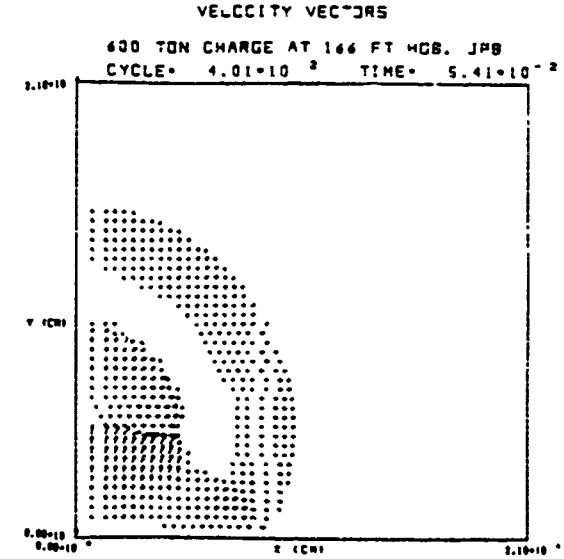

Figure 6f

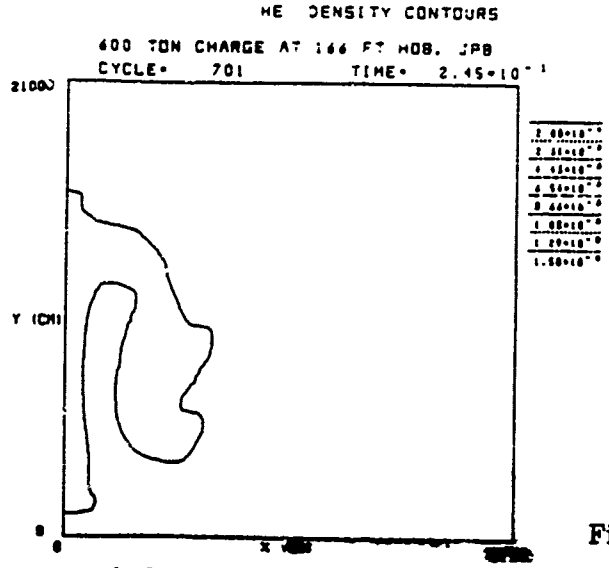

Figure 6g

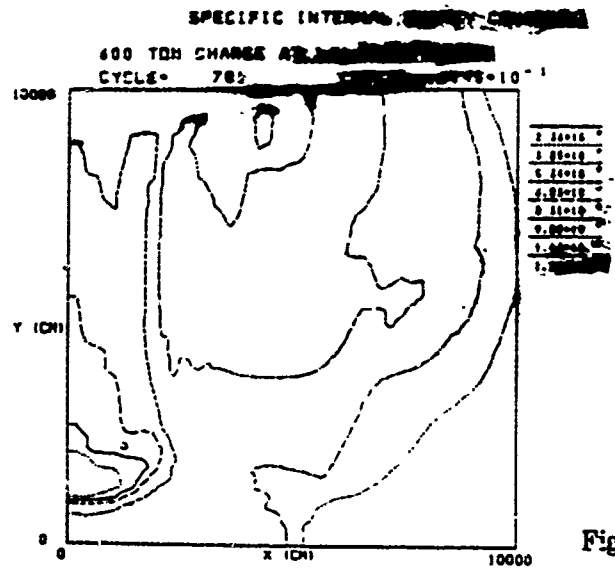

Figure 6h

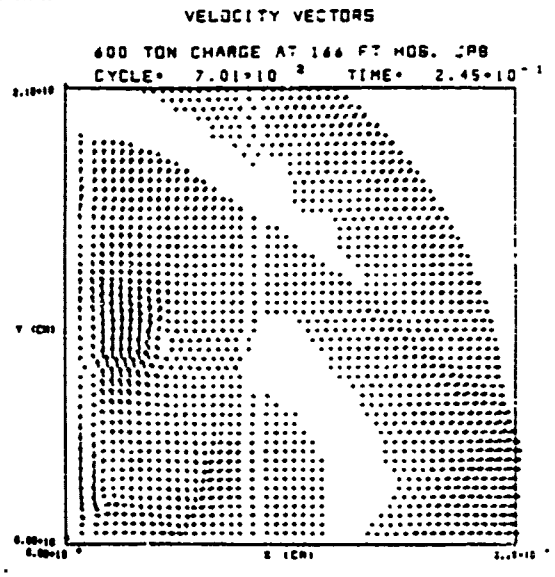

Figure 6i

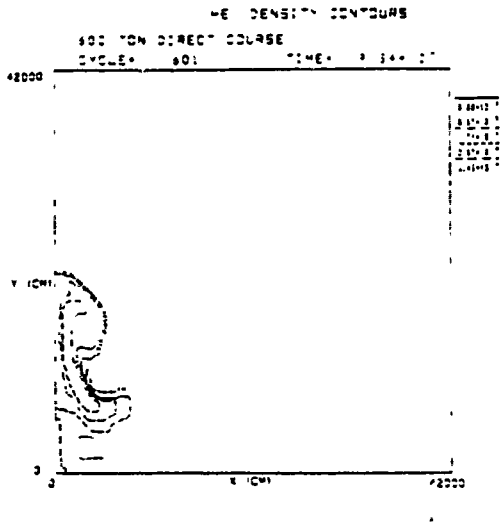

Figure 7a

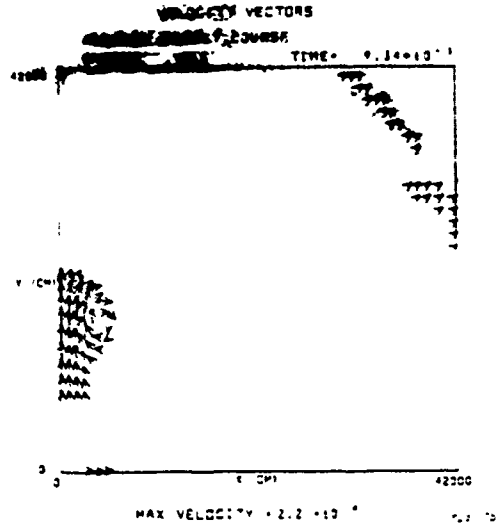

Figure 7b

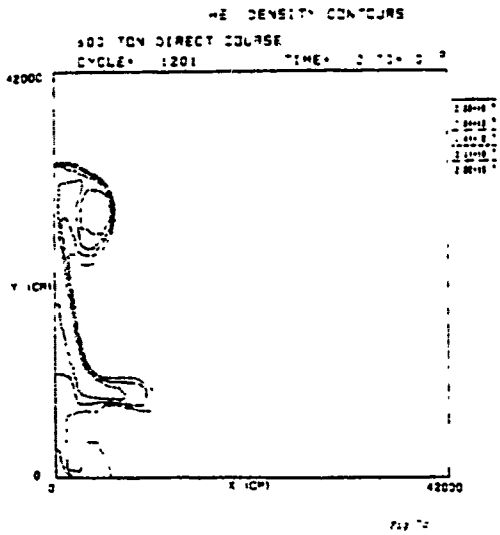

Figure 7c

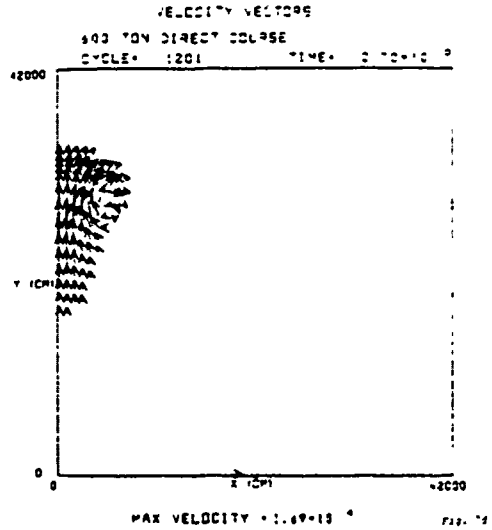

Figure 7d

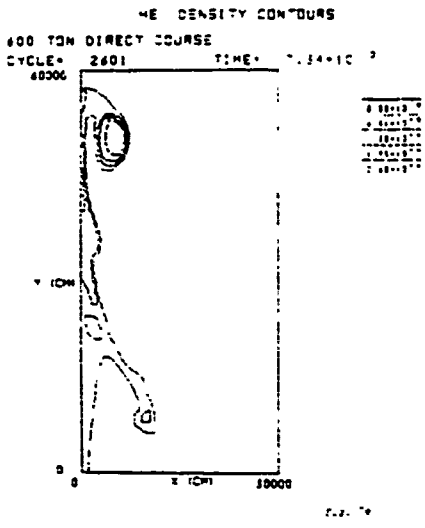

Figure 7e

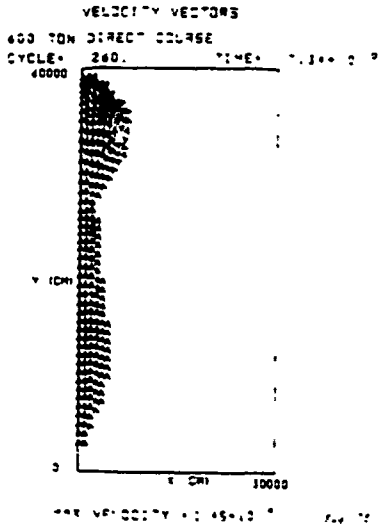

Figure 7f

even clearer. The cloud has become quite elongated vertically and shows a distinct mushroom shape. Development slows as the fireball cools and velocities diminish. By 7.34 s (after 2600 timesteps) the cloud is almost at 600 m. Figures 7(e)-(f) show its form at this time. Note that the maximum velocity is now 145 m/s.

Figure 8a, which shows the trajectories of passively advected tracer particles over the time interval 1.8 sec to 3.97 sec, displays the vortices very clearly. Figure 8b shows the particle paths for the time interval 3.97 sec to 7.34 sec. Notice that there are four vortices visible in the plot: two positive and two reversed. The additional small vortices are apparently a consequence of entrainment by the major ones. As far as we know, their existence has not been noted previously.

When we repeat the calculation with nuclear initial conditions, several differences appear at a very early stage. The reflected shock propagates upward rapidly through the much hotter fireball and reverberates more. The maximum flow speeds (as opposed to sound speeds) are smaller, a difference which persists to late times. Although the shock radius as a function of time is essentially the same, the rarefaction wave moves faster as the deeper density well gets filled in.

Figures 9(a)-(c) show plots analogous to those of Figures 6(g)-(i); by this time it is clear that much of the early difference in the density profiles is washed out as pressure begins to relax to ambient. (The pressure differs from ambient by < 5% everywhere, so that pressure contour plots are not very informative.) Note, however, the indentations that appear on the underside of the internal energy

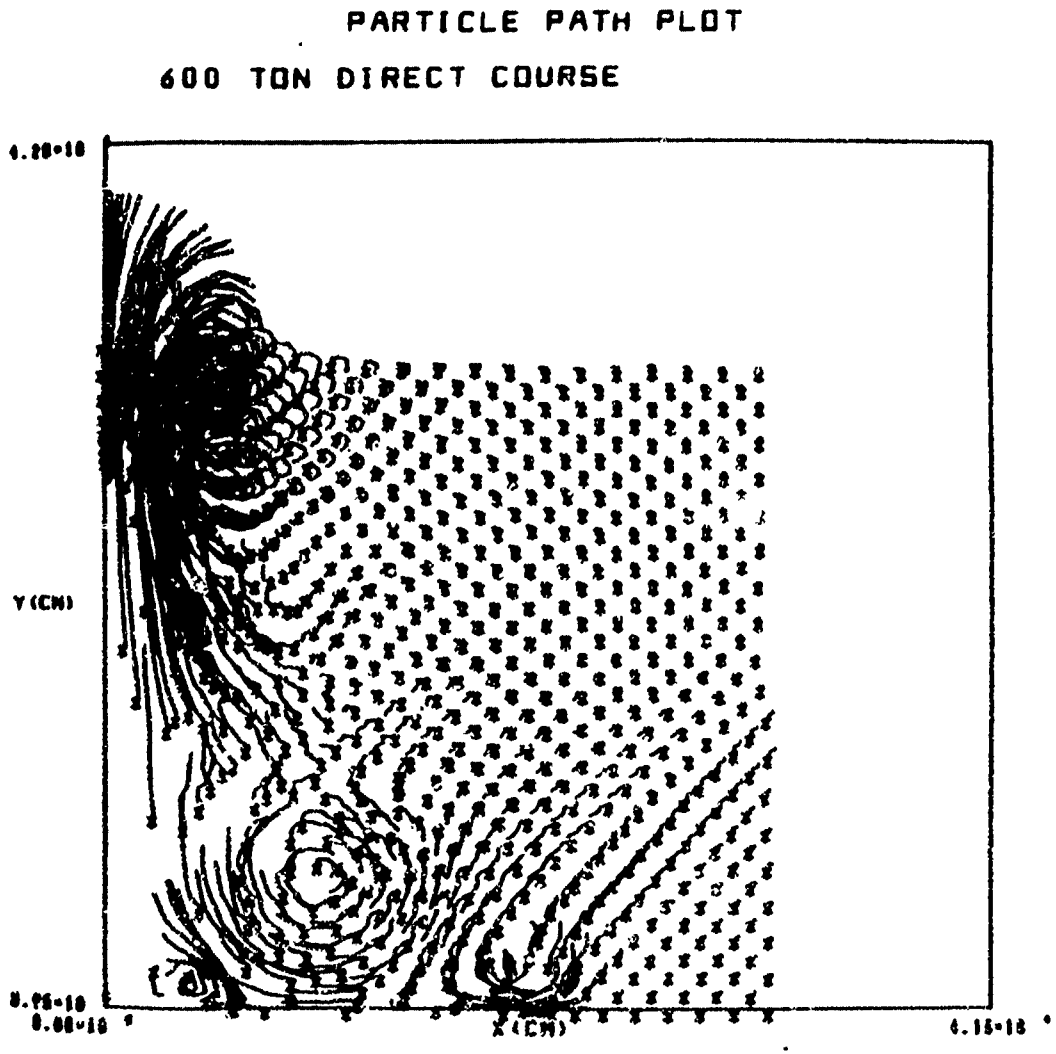

Time Interval
1.8 sec → 3.97 sec

Figure 8a

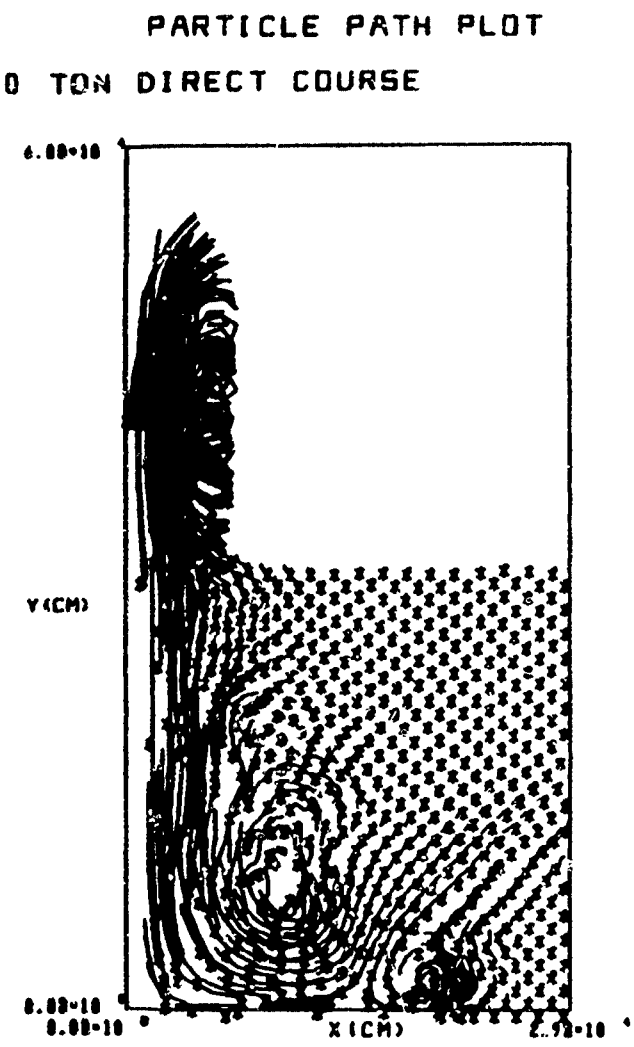

Time Interval
3.97 → 7.3 sec

Figure 8b

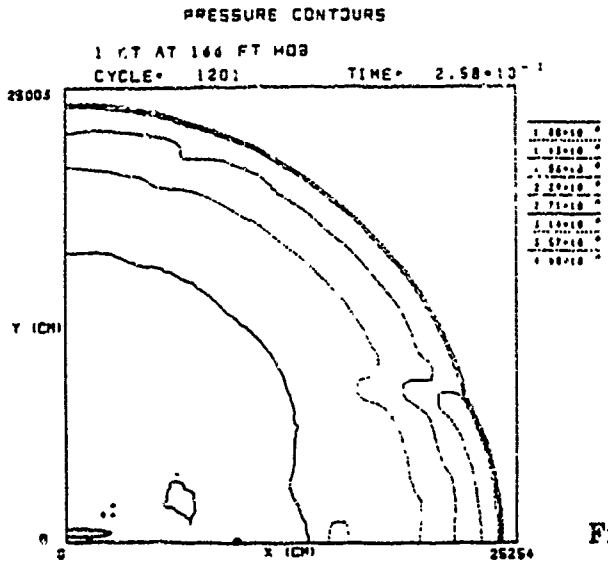

Figure 9a

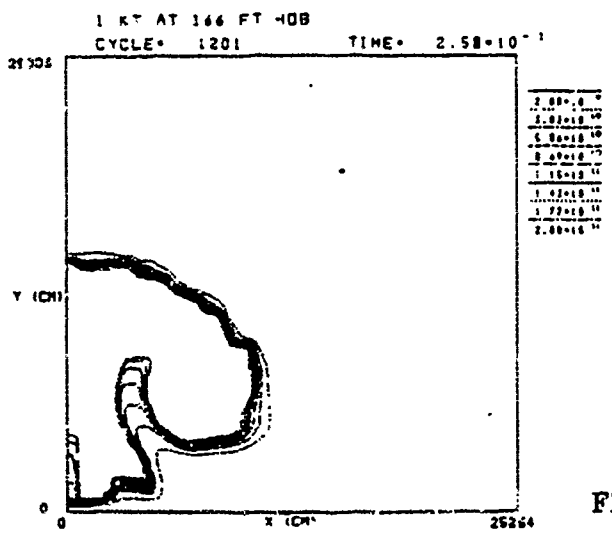

Figure 9b

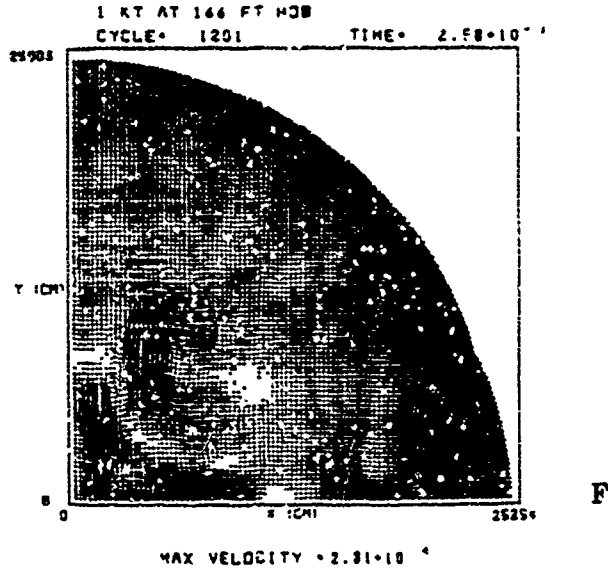

Figure 9c

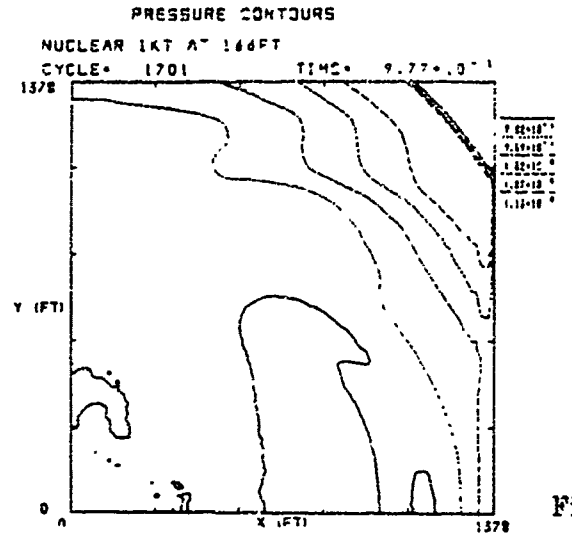

Figure 9d

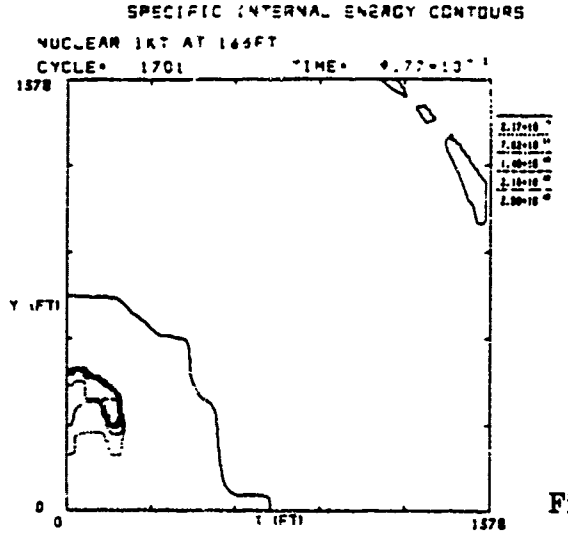

Figure 9e

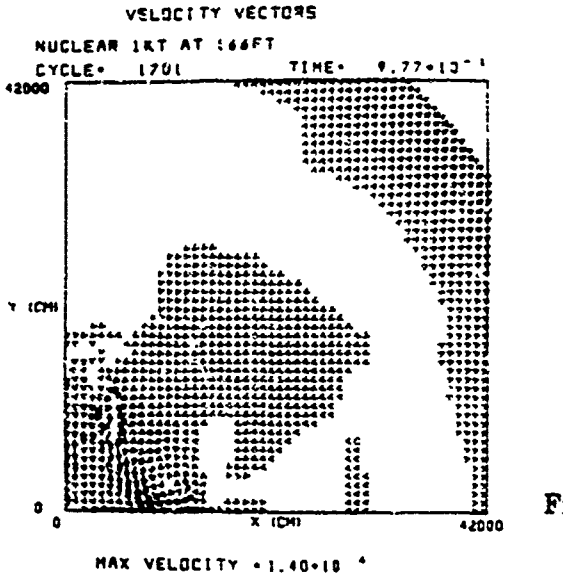

Figure 9f

contours at the base of the stem [Fig. 9(b)]. These are absent in the corresponding HE plot, Fig. 6(g). We conjecture that they are the signature of a fluid instability, possible Rayleigh-Taylor. The idea is that the air sucked in by the (forward) vortex at the bottom of the fireball is much denser than the fireball itself. In running into the latter it sets up the classic condition for Rayleigh-Taylor instability (direction of effective gravity and density gradient are opposed).

It is clear that the major qualitative differences between the HE and nuclear cases persist longest in the velocity plots. This is not surprising, as the circulation patterns represented by the vortices have essentially infinite lifetimes in the absence of viscosity. We have run both nuclear and HE cases out to stabilization (not shown here) and have shown that there are qualitative differences in velocity plots to the very end. At all times $t>0$ the peak flow velocity in the HE case exceeds that in the comparable nuclear result. This is a reflection of the fact that the Chapman-Jouguet solution at a radius of 10 m has a pressure peak of 52 kbar, vs 3 kbar for the 1-kton standard at the same radius. The means that the former starts out with much more violent motion, i.e., fluid velocities an order of magnitude larger. In point of fact, the HE case does not closely resemble a point source. At initialization the nuclear profiles have ~ 6% of the yield in kinetic energy. This fraction increases to a maximum of ~ 15%, then decreases. In the HE case the fraction is initially about one-half and decreases monotonically thereafter at about the same rate as in the nuclear case.

Section 5
CONCLUSIONS

We have described numerical simulations carried out for a 600-ton HE burst and a 1-kton nuclear burst, both at 166 ft. The code, gridding, and method of solution are the same in the two calculations. Although the shock waves in the two cases propagate at roughly the same speed and break away at roughly the same time, and although the pressure fields relax to ambient in similar fashion, we find significant differences, of which the following appear to be the most important.

(i) The HE flow velocities are systematically larger.

(ii) In the regular reflection region (underneath and close to the fireball), the HE case exhibits two overpressure peaks at the surface, rather than one, due to re-reflection of the reflected shock from the contact surface between air and detonation products.

(iii) For the HE case the upper vortex forms first, followed by the reverse vortex near the axis of symmetry and the ground. Adjacent HE products begin to be entrained into a positive vortex over a longer period of time, several seconds. In the nuclear case the negative vortex is the dominant one; it is larger then the HE, persists longer, and

contains larger velocities than the positive vortex at comparable times.

(iv) The HE flow establishes a pattern of four vortices, two forward and two reversed, instead of one of each.

(v) The stem of the nuclear fireball appears to exhibit a Rayleigh-Taylor instability, absent in the HE case.

Since the velocities on axis are higher in the HE case (the upper positive vortex is larger), fireball rise is faster than in the nuclear case. The nuclear case, however, probably scours up more dust because the velocities are larger, and the reverse vortex is larger and more persistent. It is difficult to argue conclusively on this point because so much depends on terrain, conditions in the boundary layer, and other physical effects not included in this model (e.g., precursor heating and turbulence). Further study of the tracer particle motions we have calculated is expected to be illuminating in this regard.

REFERENCES

1. Boris, J. P. and Book, D. L. in Methods in Computational Physics, J. Killeen Ed., (Academic Press, NY, 1976), Vol. 16, p. 85.

2. Boris, J. P., "Flux-Corrected Transport Modules for Solving Generalized Continuity Equations", NRL Memo Report 3237 (1976). AD-A023-891.

3. Kuhl, A. L., Fry, M. A., Picone, M., Book, D. L., Boris, J. P., "FCT Simulation of HOB AIRBLAST Phenomena", NRL Memo Report No. 4613 (1981). AD-A107 920.

4. Young, T. R., "Table Look-Up: An Effective Tool on Vector Computers", Tenth Conf. on Numerical Simulation of Plasmas, San Diego, CA, January 4-6, 1983.

5. Needham, C. E. and Crepeau, J. E., "The DNA Nuclear Blast Standard (1-KT)", DNA Report 5648T, January 1981.

6. Sedov, L. I., Similarity and Dimensional Methods in Mechanics, Academic Press, NY, 1959.

ACKNOWLEDGMENT

This work was supported by the Defense Nuclear Agency under Subtask N99QAXAH Work Unit # 00061, Work Unit Title 'Cloud Calculations".

DISTRIBUTION LIST

Assistant to the Secretary of Defense
(Atomic Energy)
Washington, DC 20301
01CY Attn Executive Assistant

Director
Defense Communications Agency
Washington, DC 20305
(ADR CNWDI: Attn Code 240 FOR)
01CY Attn Code 670 R LIPP

Director
Defense Intelligency Agency
Washington, DC 20301
01CY Attn RDS-3A (Tech LIB)
01CY Attn DB-4N
01CY Attn DT-1C
01CY Attn DT-2
01CY Attn DB-4C E Ofarrell

Director
Defense Nuclear Agency
Washington, DC 20305
02CY Attn SPSS
01CY Attn SPSS C Ullrich
01CY Attn SPSS T Deevy
04CY Attn Titl

Defense Technical Information Center
Cameron Station
Alexandria, VA 22314
(12 If open pub, otherwise 2
Nc Wnintel)
12CY Attn DD

Universal Analytics, Inc.
7740 W Manchester Blvd
Playa Del Rey, Ca 90291
01CY Attn E Field

Weidlinger Assoc. Consulting Engineers
110 E 59th Street
New York, NY 10022
01CY Attn I Sandler
01CY Attn M Baron

Weidlinger Assoc. Consulting Eng.
3000 Sand Hill Road
Menlo Park, CA 94025
01CY Attn J Isenberg

Naval Research Laboratory
Laboratory for Computational Physics
Code 4040
Washington, DC 20375
100copies Attn J Boris

Terra Tek, Inc.
420 Wakara Way
Salt Lake City, LT 84108
01CY Attn A Abou-Sayed
01CY Attn Library
01CY Attn A Jones
01CY Attn S Green

Tetra Tech, Inc.
630 N Rosemead Blvd
Pasadena, CA 91107
01CY Attn L Hwang

TRW Defense & Space Sys Group
One Space Park
Redondo Beach, CA 90278
01CY Attn N Lipner
01CY Attn Technical Info Center
01CY Attn T Mazzola

TRW Defense & Space Sys Group
P.O. Box 1310
San Bernardino, CA 92402
01CY Attn G Hulcher
01CY Attn P Dai
01CY Attn E Wong
01CY Attn Library
01CY Attn J Colton

Systems, Science & Software Inc.
P.O. Box 8243
Albuquerque NM 87198
01CY Attn C Needham

Systems, Science & Software, Inc.
P.O. Box 1620
La Jolla, CA 92038
01CY Attn J Barthel
01CY Attn T Riney
01CY Attn D Grine
01CY ATtn Library
01CY Attn C Hasting
01CY Attn K Pyatt
01CY Attn C Dismukes
01CY Attn T Cherry

Science Application, Inc
101 Continental Blvd
FL Segundo, CA 90245
01CY Attn D Hove

Science Applications, Inc.
P.O. Box 1303
McLean, VA 22102
01CY Attn J Cockayne
01CY Attn E Chambers III
01CY Attn M Knasel
01CY Attn W Layson
01CY Attn B Sievers

SRI International
333 Ravenswood Ave
Menlo Park, CA 94025
01CY Attn G Abrahamson
01CY Attn J Thompson
01CY Attn F Sauer

Rand Corp
1700 Main Street
Santa Monica, CA 90406
01CY Attn C Mow

Science Application, Inc.
P.O. Box 2351
La Jolla, CA 92038
01CY Attn H Wilson
01CY Attn Technical Library
01CY Attn R Schlaug

Pacific-Sierra Research Corp
Washington Operations
1401 Wilson Blvd
Suite 1100
Arlington, VA 22209
01CY Attn D Gormley

Systems, Science & Software, Inc.
11800 Sunrise Valley Drive
Reston, VA 22091
01CY Attn J Murphy

Teledyne Brown Engineering
Cummings Research Park
Huntsville, AL 35807
01CY Attn J Ravenscraft
01CY Attn J McSwain

Science Applications, Inc
2450 Washington Avenue
San Leandro, CA 94577
01CY Attn D Bernstein
01CY Attn D Maxwell

Southwest Research Institute
P.O. Drawer 28510
San Antonio, TX 78284
01CY ATtn A Wenzel
01CY Attn W Baker

R&D Associates
P.O. Box 9695
Marina Del Rey, CA 90291
01CY Attn R Port
01CY Attn A Kuhl
01CY Attn J Lewis
01CY Attn W Wright
01CY Attn J Carpenter
01CY Attn Technical Info Center

Sicence Applications, Inc.
Radiation Instrumentation Div
4615 Hawkins, NE
Albuquerque, NM 87109
01CY Attn J Dishon

Pacific-Sierra Research Corp
1456 Cloverfield Blvd
Santa Monica, CA 90404
01CY Attn H Brode

Pacifica Technology
P.O. Box 148
Del Mar, CA 92014
01CY Attn R B Jork
01CY Attn G Kent
01CY Attn Tech Library

Patel Enterprises, Inc
P.O. Box 3531
Huntsville, AL 35810
01CY Attn M Patel

Physics International Co
2700 Merced Street
San Leandro, CA 94577
01CY Attn L Behrmann
01CY Attn Technical Library
01CY Attn E Moore

McDonnell Douglas Corp
5301 Bolsa Avenue
Huntsville Beach, CA 92647
01CY Attn H Herdman
01CY Attn R Halprin
01CY Attn D Dean

McDonnell Douglas Corp
3855 Lakewood Boulevard
Long Beach, CA 90846
01CY Attn M Potter

Merritt Cases, Inc.
P.O. Box 1206
Redlands, Ca 92373
01CY Attn J Merritt
01CY Attn Library

Meteorology Research, Inc.
464 W Woodbury Rd
Altadena, CA 91001
01CY Attn W Green

Mission Research Corp.
P.O. Drawer 719
Santa Barbara, CA 93102
(All class: Attn: SEC Ofc For)
01CY Attn C Longmire
01Cy Attn G McCartor

Kaman Sciences Corp.
P.O. Box 7463
Colorado Springs, CO 80933
01CY Attn D Sachs
01CY Attn F Shelton
01CY Attn Library

Kaman Tempo
816 State St (P.O. Drawer QQ)
Santa Barbara, CA 93120
01CY Attn Dasiac

Lockheed Missiles & Space Co. Inc.
P.O. Box 504
Sunnyvale, CA 94086
01CY Attn J Weisner
01CY Attn Technical Library

Martin Marietta Corp
P.O. Box 5837
Orlando, FL 32855
01CY Attn G Fotibo

Martin Marietta Corp
P.O. Box 179
Denver, CO 80201
01CY Attn G Freyer

Information Science Inc.
123 W. Padre Street
Santa Barbara, CA 93105
01CY Attn W Dudziak

Institute for Defense Analyses
400 Army-Navy Drive
Arlington, VA 22202
01CY Attn Classified Library

J D Haltiwanger Consult Eng Svcs
RM 106A Civil Engineering Bldg
208 N Romine Street
Urbana, IL 61801
01CY Attn W Hall

J.H. Wiggins Co., Inc.
1650 S Pacific Coast Highway
Redondo Beach, CA 90277
01CY Attn J Collins

Kaman Avidyne
83 Second Avenue
Northwest Industrial Park
Burlington, MA 01803
01CY Attn R Ruetenik
01CY Attn Library
01CY Attn N Hobbs
01CY Attn E Criscione

General Research Corp
Santa Barbara Division
P.O. Box 6770
San Barbara, CA 93111
01CY Attn TIO

IIT Research Institute
10 W 35th Street
Chicago, Il 60616
01CY Attn R Welch
01CY Attn M Johnson
01CY Attn Documents Library

EG&G Wash. Analytical Svcs Ctr, Inc.
P.O. Box 10218
Albuquerque, NM 87114
01CY Attn Library

Gard, Inc.
7449 N Natchez Avenue
Niles, Il 60648
01CY Attn G Neidhardt (uncl only)

Bom Corp
P.O. Box 9274
Albuquerque, NM 87119
01CY Attn R Hensley

California Research & Technology, Inc
6269 Variel Ave
Woodland Hills, CA 91367
01CY Attn Library
01CY Attn K Kreyenhagen
01CY Attn M Rosenblatt

Calspan Corp
P.O. Box 400
Buffalo, NY 14225
01CY Attn Library

General Electric Co
Space Division
Valley Forge Space Center
P.O. Box 8555
Philadelphia, PA 19101
01CY Attn M Bortner

H Tech Labs, Inc.
P.O. Box 1686
Santa Monica, CA 90406
01CY Attn Bartenbaum

Denver University of
Colorado Seminary
Denver Research Institute
P.O. Box 10127
Denver, CO 80210
(only 1 copy of class reports)
01CY Attn Sec Officer for J Wisotski

Eric H. Wang
Civil Engineering Rsch PAC
University of New Mexico
University Station
P.O. Box 25
Albuquerque, NM 87131
01CY Attn J Lamb
01CY Attn P Lodde
01CY Attn N Baum
01CY Attn J Kovarna

Boeing Co
P.O. Box 3707
Seattle, Washington 98124
01CY Attn S Strack
01CY Attn Aerospace Library
01CY Attn M/S 42/37 R Carlson

California Research & Tech Inc.
4049 First Street
Livermore, CA 94550
01CY Attn D Orphal

Applied Theory, Inc.
1010 West Wood Blvd
Los Angeles, CA 90024
(2 Cys if unclass or 1 Cy if Class)
01CY Attn J Trulio

APTEC Associates in Inc.
26046 Eden Landing Road
Hayward, CA 94545
01CY Attn S Gill

AVCO Research & Systems Group
201 Lowell Street
Wilmington, MA 01887
01CY Attn Library A830

ACUREX Corp.
485 Clyde Avenue
Mountain View, CA 94042
01CY Attn C Wolf

Agbabian Associates
250 N Nash Street
El Segundo, CA 90245
01CY Attn M Agbabian

Applied Research Associates, Inc.
2601 Wyoming Blvd NE Suite H-1
Albuquerque, NM 87112
01CY Attn J Bratton
01CY Attn N Higgins

Department of the Interior
Bureau of Mines
Bldg 20, Denver Federal Center
Denver, CO 80225
(Unclasified Only)
01CY Attn Tech Library

Sanida National Lab
P.O. Box 5800
Albuquerque, NM 87185
All Class Attn Sec Control OFC FOR
01CY Attn A Chaban
01CY Attn L Hill
01CY Attn Org 1250 W Brown
01CY Attn A Chabia
01CY Attn W Roherty
01CY Attn 3141
01CY Attn L Vortman
01CY Attn J Banister

Astron Research & Engineering
1901 Old Middlefield Way #15
Mountain View, CA 94043
01CY Attn J Huntington

BDM Corp.
7915 Jones Branch Drive
McLean, VA 22102
01CY Attn A Lavagnino
01CY Attn T Neighbors
01CY Attn Corporate Library

Aerospace Corp.
P.O. Box 92957
Los Angeles, CA 90009
01CY Attn H Mirels
01CY Attn Technical Info Services

Analytic Services, Inc.
400 Army-Navy Drive
Arlington, VA 22202
01CY Attn G Hesselbacher

Central Intelligence Agency
Washington, DC 20505
01CY Attn OSWR/NED

Director
Federal Emergency Management Agency
Natinal Sec Ofc Mitigation & Rsch
1725 I Street NW
Washington, DC 20472
(All class attn B105 DOC Control FOR
01CY Attn Mitigati n & Rsch Div.

Los Alamos National Scientific Lab
Mail Station 5000
P.O. Box 1663
Los Alamos, NM 87545
Classified only to mail station 5000
01CY Attn R Whittaker
01CY Attn C Keller
01CY Attn M.T. Sanford
01CY Attn MS 364 (Class Reports LIB
01CY Attn E Jones

Lovelace Biomedical & Environment
Rsch Institute, Inc.
P.O. Box 5890
Albuquerque, NM 87115
01CY Attn R Jones (uncl only)

Sandia Laboratories
Livermore Laboratory
P.O. Box 969
Livermore, CA 94550

Department of Energy
Washingotn, Dc 20545
01CY Attn OMA/RD&T

Lawrence Livermore National Lab
P.O. Box 808
Livermore, CA 94550
01CY Attn L-90 R Dong
01CY Attn L-250 J Hearst (Class L-203)
01CY Attn L-90 D Norris (Class L-504)
01CY Attn L-7 J Kahn
01CY Attn D Glenn
01CY Attn L-437 R Schock
01CY Attn Technical Info Dept Library
01CY Attn L-200 T Bltkovich

Vela Seismological Center
312 Montgomery Street
Alexandria, VA 22314
01CY Attn G Ullrich

Assistant Chief of Staff
Intelligence
Department of the Air Force
Washington, DC 20330
01CY Attn In Rm 4A932

Oak Ridge National Laboratory
Nuclear Division
X-10 Lab Records Division
P.O. Box X
Oak Ridge, TN 37830
01CY Attn Civil Def Res Proj
01CY Attn Att Central Rsch Library

Department of Energy
Albuquerque Operations Office
P.O. Box 5400
Albuquerque, NM 87115
01CY Attn CTID

Department of Energy
Nevada Operations Office
P.O. Box 14100
Las Vegas, NV 89114
01CY Attn Mail & Records for
Technical Library

Commander
Rome Air Development Center AFSC
Griffiss AFB, NY 13441
(Desires No CNWDI)
01CY Attn TSLD

Strategic Air Command
Department of the Air Force
Offutt AFB, NB 68113
01CY Attn NRI-Stinfo Library
01CY Attn XPFS
01CY Attn Int J McKinney

Director
Air University Library
Department of the Air Force
Maxwell AFB, AL 36112
(Desires NO CNWDI)
01CY Attn Aul-LSE

Assistant Chief of Staff
Studies & Analyses
Department of the Air Force
Washington, DC 20330
01CY Attn AF/SAMI (Tech Lib)

Assistant Secretary of the AF
Research, Development and Logistics
Department of the Air Force
Washington, DC 20330
01CY Attn SAFALR/Dep for Strat & Space Sys

Air Force Institute of Technology
Air University
Wright-Patterson AFB, OH 45433
(Does Not Desire Classified Documents)
01CY Attn Library

Air Force Weapons Laboratory, AFSC
Kirtland AFB, NM 87117
01CY Attn NTES-C R Henny
01CY Attn NTED-I
01CY Attn NTED R Matalucci
01CY Attn NTF M Plamondon
01CY Attn NT D Payton
01CY Attn NTED-A
01CY Attn NTES-G
01CY Attn SUL
01CY Attn DEX
01CY Attn NTES-S
01CY ATtn NTEO
01CY Attn DEY

Deputy Chief of Staff
Logistics & Engineering
Department of the Air Force
Washington, DC 20330
01CY Attn LEEF

Office of the Chief of Naval Operations
Washington, DC 20350
01CY Attn OP 981
01CY Attn OP 03EG

Commander
Naval Surface Weapons Center
Dahlgren, VA 22449
01CY Attn Tech Library & Info Svcs Br

Commander
Naval Weapons Center
China Lake, CA 93555
01CY Attn Code 3201 P Cordle
01CY Attn Code 266 C Austin
01CY Code 233 (Tech Lib)

Air Force Geophysics Laboratory
Hanscom AFB, MA 01731
01CY Attn LWW K Thompson

Headquarters
Air Force Systems Command
Andrews AFB, DC 20334
01CY Attn DLWM
01CY Attn DLW

Ballistic Missile Office/MN
Air Force Systems Command
Norton AFB, CA 92409
(Minuteman)
01CY Attn MNNXH G Kalansky
01CY Attn MNNXH M Delvecchio
01CY Attn MNN W Crabtree
01CY Attn MNNXH D Gage
01CY Attn MNNX

Deputy Chief Staff
Research, Development & ACQ
Department of the Air Force
Washington, DC 20330
01CY Attn AFRDQI N Alexandrow
01CY Attn AFRDPN
01CY Attn AFRDQI

Commander
Foreign Technology Division, AFSC
Wright-Patterson AFB, OH 45433
01CY Attn NIIS Library

Director
Strategic Systems Project Office
Department of the Navy
Washington, DC 20376
01CY Attn NSP-272
01CY Attn NSP-43 (Tech Lib)

President
Naval War College
Newport, RI 02840
01CY Attn Code E-11 (Tech Service)

Commanding Officer
Naval Weapons Evaluation Facility
Kirtland Air Force Base
Albuquerque, NM 87117
01CY Attn R Hughes
01CY Attn Code 10 (Tech Lib)

Office of Naval Research
Arlington, VA 22217
01CY Attn Code 474 N Perrone

Superintendent
Naval Postgraduate School
Monterey, CA 93940
(Desires No CNWDI Documents)
01CY Attn Code 1424 Library
01CY Attn G Lindsay

Commander
Naval Sea Systems Command
Washington, DC 20362
01CY Attn SEA 09G53 (Lib)
01CY Attn SEA 0351

Commander
David Taylor Naval Ship R&D Ctr
Bethesda, MD 20084
(CNWDI only Attn Mrs. M Birkhead
Code 5815.6)
01CY Attn Code L42-3 (Library)

Commander
Naval Electronic Systems Command
Washington, DC 20360
01CY Attn PME 117-21

Headquarters
Naval Material Command
Washington, DC 20360
01CY Attn MAT 08T-22

Commander
U.S. Army Mobility Equip R&D CMD
Fort Belvoir, VA 22060
(CNWDI to Army MAT Dev & Readiness Com
01CY Attn Drome-WC (Tech Lib)

Commander
Naval Ocean Systems Center
San Diego, CA 92152
01CY Attn Code 013 E Cooper
01CY Attn Code 4471 (Tech Lib)

Commanding Officer
Naval Research Laboratory
Washington, DC 20375
(RD & RD/N Attn Code 1221 for &
FRD Attn Code 2628 FOR)
01CY Attn Code 4040 J Boris
01CY Attn Code 2627 (Tech Lib)
01CY Attn 4040 D Book

Officer in Charge
Naval Surface Weapons Center
White Oak Laboratory
Silver Spring, MD 20910
01CY Attn P44 H Galz
01CY Attn Code F31
01CY Attn Code X211 (Tech Lib)

Office in Charge
Naval Civil Engineering Laboratory
Port Hueneme, CA 93041
01CY Attn Code L53 Forrest
01CY Attn Code L08A Library
01CY Attn Code L51 J Crawford
01CY Attn L51 R Murtha

Commander
Naval Facilities Engineering Command
Washington, DC 20390
01CY Attn Code 04B

Commander
U.S. Army Missile Command
Redstone Arsenal, AL 35898
01CY Attn RSIC
01CY Attn DRDMI-XS

Commander
U.S. Army Nuclear & Chemical Agency
7500 Backlick Road
Building 2073
Springfield, VA 22150
(Desires only 1 cy to library)
01CY Attn J Simms
01CY Attn Library

Commandant
US Army War College
Caplisle Barracks, PA 17013
01CY Attn Library

Commander
US Army Foreign Science & Tech Ctr
220 7th Street, NE
Charolttesville, VA 22901
01CY Attn DRXST-SD

Commander
US Army Material Dev & Readiness CMD
5001 Eisenhower Avenue
Alexandria, VA 22333
01CY Attn DRCDE-DL Flynn
01CY Attn DRXAM-TL (Tech Lib)uncl only

Director
US Army construction Energe Res Lab
P.O. Box 4005
Champaign, IL 61820
01CY Attn Library

Division Engineer
US Army Engineer Div Huntsville
P.O. Box 1600, West Station
Huntsville, AL 35807
01CY Attn Hnded-SR
01CY Attn Hnded-FD

Commander
US Army Armament Material Readiness Com
Rock Island, IL 61202
01CY Attn MA Library

Commander and Director
US Army Cold Region Res Engr Lab
P.O. Box 282
Hanover, NH 03755
01CY Attn Library

Director
US Army Eng Waterways Exper Station
P.O. Box 631
Vicksburg, MS 39180
01CY Attn J Zelasko
01CY Attn Wessd J Jackson
01CY Attn J Strange
01CY Attn Wesse L Ingram
01CY Attn Library
01CY Attn Wessa W Flathau

Commander
US Army Material & Mechanics Rsch Ct
Watertown, MA 02172
(Address CNWDI: Attn Document
Control FOR:)
01CY Attn Technical Library
01CY Attn DRXMR-TE R Shea
01CY Attn DRXMR J Mescall

Commander
US Army Concepts Analysis Agency
8120 Woodmont Avenue
Bethesda, MD 20014
01CY Attn CSSA-ADL (Tech Lib)

Commander
US Army Engineering Center
Fort Belvoir, VA 22060
01CY Attn Technical Library
01CY Attn ATZA

Commander
Harry Diamond Laboratories
Department of the Army
2800 Powder Mill Road
Adelphi, MD 20783
(CNWDI-Inner Envelope-Attn: Delhd-
Rbh FOR)
01CY Attn DELHD-I-TL (Tech Lib)
01CY Attn Chif Div 20000

Director
US Army Ballistic Research Labs
Aberdeen Proving Ground, MD 21005
01CY Attn DRDAR-BLV
01CY Attn DRDAR-BLT J Keefer
01CY Attn DRDAR-TSB-S (Tech Lib)

Dep Ch of Staff FOR OPS & Plans
Department of the Army
Washington DC 20310
01CY Attn DAMO-NC

Director
BMD Advanced Technology Center
Department of the Army
P.O. Box 1500
Huntsville, AL 35807
01CY Attn ATC-T
01CY Attn ICRDABH-x
01CY Attn ATC-T

Commander
BMD Systems Command
Department of the Army
P.O. Box 1500
Huntsville, AL 35807
01CY Attn BMDSC-HW
01CY Attn BMDSCH-HW R Dekalb
01CY Attn BMDSCH H N Hurst
01CY Attn BMDSCH RC Webb

Chief of Engineers
Department of the Army
Forrestal Building
Washington, DC 20314
01CY Attn DAEN-MCE-D
01CY Attn DAEN-RDL
01CY Attn DAEN-MPE-T D Reynolds

Commandant
NATO School (SHAPE)
APO New York 09172
01CY Attn US Documents Officer

Under Secy of Def For Rsch & Engrg
Department of Defense
Washington, DC 20301
01CY Attn Strategic & Space Sys
Rm. 3E129

Chairman
Department of Defense Explo Safety
Board
2461 Eisenhower Avenue
Alexandria, VA 22331
01CY Attn Chairman

Commander
Field Command
Defense Nuclear Agency
Kirtland AFB, NM 87115
01CY Attn FCTMOF
01CY Attn FCT
01CY Attn FCPR
01CY Attn FCTT

Chief
Field Command
Defense Nuclear Agency
Livermore Branch
P.O. Box 808 L-317
Livermore, CA 94550
01CY Attn FCPRL

Director Joint Strat TGT Planning Staff
OFFUTT AFB
Omaha, NB 68113
01CY Attn JLA
01CY Attn DOXT
01CY Attn XPES
01CY Attn NRI-STINFO Library
01CY ATtn JLTW-2

Horizons Technology, Inc.
7830 Clairement Mesa Blvd
San Diego, CA 92111
01CY Attn R Kruger

Gard, Inc.
7449 N Natchez Avenue
Niles, IL 60648
01CY Attn G Neidhardt (uncl only)